行政院國家科學委員會補助專題研究計畫 ■成果報告 □期中進度報告

微孔多階衝擊器之研發

計畫類別：■ 個別型計畫　□ 整合型計畫
計畫編號：NSC 98－2221－E－009－020－MY3
執行期間：99 年 8 月 1 日至 101 年 7 月 31 日

計畫主持人：蔡春進
共同主持人：
計畫參與人員：陳聖傑、劉俊男、洪毅弘、Amit Awasthi
成果報告類型(依經費核定清單規定繳交)：□精簡報告 ■完整報告

本成果報告包括以下應繳交之附件：
□赴國外出差或研習心得報告一份
□赴大陸地區出差或研習心得報告一份
■出席國際學術會議心得報告及發表之論文各一份
□國際合作研究計畫國外研究報告書一份

處理方式：除產學合作研究計畫、提升產業技術及人才培育研究計畫、列管計畫及下列情形者外，得立即公開查詢
□涉及專利或其他智慧財產權，□一年■二年後可公開查詢

執行單位：國立交通大學環境工程研究所

中　華　民　國　101　年　10　月　23　日

摘要

本研究主要針對使用微孔多階衝擊器時常會產生的問題進行探討或解決，分別是固體微粒彈跳、噴嘴阻塞以及微粒損失。在固體微粒彈跳方面，本研究探討大氣相對濕度和未塗敷矽油之衝擊基質上固體微粒彈跳之間的關係。結果顯示微粒彈跳隨溼度的降低而愈趨嚴重，而無塗敷的鋁箔比無塗敷的鐵氟龍嚴重。當相對溼度介於 40-80%，微粒彈跳並不會影響整個大氣細微粒的質量分佈，不過卻會嚴重的低估大於 2.5 μm 的微粒濃度。當相對濕度降低至 50 及 25%，使用不塗敷鋁箔及鐵氟龍的 MOUDI 會分別過度採集 $PM_{0.1}$ 質量達 95-180%及 25-50%。而當分別控制 RH 在大於 75 及 65%時，無塗敷鋁箔及無塗敷鐵氟龍 MOUDI 可明顯降低微粒彈跳的情形且可準確的採集 $PM_{0.1}$ 在 5%的誤差以內。

除了微粒彈跳之問題之外，MOUDI 下方階層之噴嘴片在使用後也常會有噴嘴阻塞的現象。為解決此問題，本研究開發出了一部 NCTU 微孔多階衝擊器 (NCTU, Micro-Orifice Cascade Impactor, NMCI)。NMCI 為一個其第 7 至 10 階衝擊器被換上新型噴嘴片的 10 階 MOUDI，該新型噴嘴片係由 LIGA (Lithography, Electroplating, and Molding)製程所製造，其噴嘴內壁的形狀呈平滑狀，預期較不易產生微粒阻塞的情況。為了評估其採樣能力，本研究會先針對 MOUDI 及 NMCI 進行微粒收集效率曲線的校正並量測其內部奈米微粒的損失。測試結果顯示，當兩者衝擊器的 S/W 比值(S:噴嘴至衝擊板之距離，W: 噴嘴直徑)調整至適當值後，其第 7 至 10 階衝擊器的截取氣動直徑(d_{pa50})會和 Marple et al. (1991)論文中的設計值相當接近。從進口端至第 6 到第 10 階的總微粒損失會因為對流擴散沉降而導致此損失會隨著微粒粒徑降低而增加。在 MOUDI 中，總微粒損失會由進口端至第 6 階的 2.9 至 15.3 % (d_{pa}: 105.8 至 15.4 nm)增至由進口端至第 10 階的 20.1 至 26.1 % (d_{pa}: 23 至 15.4 nm)。相近但略低上述數值的損失也存在於 NMCI 中。現場比對測試的結果顯示兩者所測得的微粒質量粒徑分布相似。最後，利用高濃度燻煙進行採樣的噴嘴阻塞測試實驗則顯示，相較於 MOUDI，NMCI 的噴嘴較不易產生堵塞的情形。

關鍵字: 多階慣性衝擊器、固體微粒彈跳、氣膠採樣、相對溼度、奈米微粒、噴嘴阻塞、微粒損失

ABSTRACT

This study is aimed to investigate or solve the practical problems when using the cascade impactors including solid particle bounce, nozzle clogging and interstage loss. For solid particle bounce, the effect of ambient relative humidity (RH) on solid particle bounce from the uncoated impaction substrate was investigated. Results showed that decreasing RH in general increased particle bounce from uncoated substrates with the bounce from uncoated aluminum foils (ALs) being more severe than from Teflon filters (TFs). Particle bounce did not influence the overall mass distribution of ambient fine particles when RH ranged between 40 to 80 % while it severely under-sampled particles greater than 2.5 μm in aerodynamic diameter. Oversampling of $PM_{0.1}$ by as much as 95-180 % or 25-50 % occurred when the MOUDI used uncoated ALs or TFs, respectively, as RH was reduced from 50 to 25%. Particle bounce was reduced substantially and $PM_{0.1}$ was found to be sampled accurately with less than 5 % of error by the MOUDIs with uncoated ALs and TFs at the RH > 75 and 65 %, respectively.

In addition to particle bounce, the other practical problem is nozzle clogging. To resolve this problem, the NCTU micro-orifice cascade impactor (NMCI) was developed. In the NMCI, new nozzle plates with smooth nozzle shape made by the LIGA (Lithography, Electroplating, and Molding) process were used to replace the 7^{th} to 10^{th} stages in one of the MOUDI. To evaluate the sampling performance of the NMCI, the NMCI and the MOUDI were tested for the particle collection efficiency curves and interstage loss of nanoparticles. Test results show that after adjusting proper S/W ratios (S: jet to plate distance, W: nozzle diameter), the cutoff aerodynamic diameters (d_{pa50}) are close to the nominal values given in Marple et al. (1991). Total interstage loss of nanoparticles from the inlet to the 6^{th} to 10^{th} stage of the MOUDI exists due to the convection-diffusion mechanism, which increases with decreasing d_{pa}. For the MOUDI, total loss is 2.9 to 15.3 % (d_{pa}: 105.8 to 15.4 nm) for the inlet to the 6^{th} stage and it increases to 20.1 to 26.1 % (d_{pa}: 23 to 15.4 nm) for the inlet to the 10^{th} stage, respectively. Similar but slightly lower loss also exists in the NMCI. Field comparison tests in the ambient air show that mass size distributions measured by the MOUDI agree well with those of the NMCI. Finally, nozzle clogging tests using high concentration incense smokes indicate that the NMCI has a much less tendency for particles to clog in the nozzles than the MODUI.

Keywords: cascade impactor, solid particle bounce, relative humidity, nanoparticles, nozzle clogging, particle loss.

1. Introduction

Both ambient ultrafine particles (UFPs) and engineered nanoparticles (ENPs) may pose health risks to humans when there are inhaled or ingested. Nanoparticles (NPs) induce lung injury due to their ability to generate reactive oxygen species (ROS). Using the RAW 264.7 phagocytic cell line to compare the cellular effects of ambient UFPs with four other ENPs, it was found ambient UFPs and engineered cationic polystyrene NPs showed clear evidence of cellular toxicity as compared to the other ENPs. Ambient UFPs had the additional effect of inducing pro-inflammatory responses (Xia et al., 2006). Therefore, it is important to understand the pollutant sources and adopt proper control measures to avoid human exposure to UFPs and ENPs.

Cascade impactors such as the micro-orifice uniform deposit impactor (MOUDI) (Marple et al. 1991), the low pressure impactor (LPI) (Hering et al. 1979) and the electric low pressure impactor (ELPI) (Keskinen et al. 1992) are the common device for nanoparticle sampling. Among them, the MOUDI is the most widely used device (Chow and Watson, 2007) because of its relatively smaller interstage pressure drop as compared to low pressure impactors which reduces potential evaporation of volatile aerosol species.

There are some major concerns when using cascade impactors, such as solid particle bounce and interstage loss (Marple et al. 2001). Solid particle bounced from the upper impactor stages to the lower stages with smaller cut sizes will lead to overestimations of particle mass concentrations in the lower stages. That is, this problem is more severe for submicron particles and $PM_{0.1}$ than larger PM fractions. Applying a sticky substance or low viscosity oil on the substrates was recommended to reduce bounce (Gulijk et al., 2003; Pak et al., 1992; Turner and Hering, 1987), but interference with the chemical analysis of POC (particulate organic carbon) occurs. Moreover, evaporation of oil and subsequent adsorption by filters may also occur, which create errors in determining particle mass and chemical species concentrations. Thus, uncoated substrates are normally used in field sampling studies and this might be the reason why the MOUDI oversampled $PM_{0.1}$ severely as compared to the calculated $PM_{0.1}$ concentrations of the SMPS (Khlystov et al., 2004; Shen et al., 2002).

Ambient aerosol particles are known to be hygroscopic due to the presence of inorganic salts and organic acid, leading to water vapor absorption as relative humidity increases. This suggests that sampling ambient particles at a controlled and high relative humidity (RH) condition without using coated impaction substrates is possible since liquid particles are much less bouncy than solid particles. Vasiliou et al. (1999) used a relative humidity (RH) conditioner made of 16 ceramic tubes and filled

with saturated NaCl solution to control the RH at about 75±2% of aerosol flow entering the uncoated 10 stage MOUDI (MSP Model 110) during field samplings at Las Vegas with low RHs of about 10 to 30%. The percent of sulfate mass on the after filter (or PM0.056) to the sum of all stages of the conditioned MOUDI was compared with that of a collocated unconditioned MOUDI. It was found that the bounce of fine ambient particles in the conditioned MOUDI was largely eliminated when the sampled aerosol flow was above ~70% RH. However, there was a tendency for the sulfate loading at the after filter to decrease with increasing RH. The average percent of sulfate mass on MOUDI after filter was 2 and 4%, respectively, for the conditioned and unconditioned MOUDIs, which implied that unconditioned MOUDI oversampled PM0.056 by 100%. They concluded that accurate mass distribution of ambient particles could be obtained by MOUDI when RHs were kept at above ~70% but below 80% for fear that flow-induced sizing errors might occur (Fang et al., 1991).

Stein et al. (1994) used a Tandem Differential Mobility Analyser (TDMA) with a relative humidity conditioner to study the bounce of atmospheric 0.25 μm particles in a one stage 0.1 μm cutsize impactor in which uncoated aluminum foils (ALs) were used as the impaction substrates. They found the bounce of 0.25 μm particles increased sharply as relative humidity decreased below 60-70%. At RHs of 50, 40, 30 and 20%, about 10, 20, 40 and 70% of incoming 0.25 μm particles bounced. Less than 3% of particles bounced when the relative humidity was kept at 70-80%, when the surface loading effect on bounce was also found to be negligible. Dzubay et al. (1976) studied particle bounce of larger particles in the Anderson 2000 cascade impactor which had the size cuts of 7.0, 3.3, 2.0 and 1.1 μm. In the study, two of the impactors in parallel were compared near a freeway, one of which used vacuum grease coated ALs as impaction substrates while the other used uncoated ALs. The grease coated impactor was regarded as the reference sampler. They found the MMAD (mass median aerodynamic diameter) of the uncoated impactor was 2-5 times smaller than the coated impactor due to particle bounce.

It is very important to obtain the interstage loss data when calibrating a cascade impactor, since it may result in the shift of the collection efficiency curve to the smaller particle size (Liu et al. 2011) or even lift the left tail end of the curve (Hillamo and Kauppinen, 1991). The interstage loss in the MOUDI was measured during its initial development (Marple et al. 1991). However, the loss for nanoparticles with the diameter smaller than the d_{pa50} of each of the lower stages was not tested. In addition, the loss of nanoparticle can occur in the upstream stages before a certain lower stage, which is hard to measure because the loss per stage is small unless the test is conducted from the inlet to a specific lower stage. In Virtanen et al. (2001), particles with the size from 10 to 400 nm were used to measure the loss for the 5^{th} to 12^{th} stage

of the ELPI with the corresponding d_{pa50} ranging from 260 nm to 6.7 μm. However, only particles (silver particles: 10 to 40 nm, DOS particles: 40 to 400 nm) which were smaller than d_{pa50} and deposited on the impaction plates of the stages were considered as particle loss while particles might also deposit between stages. In addition, particle loss in the lower 1st to 4th stages with d_{pa50} smaller than 260 nm was not measured.

Another practical problem needs to be addressed is particle clogging in the nozzles due to long-term or high particle concentration sampling, which may often be ignored by many users since this problem develops slowly. The clogged nozzles may result in an increase in the pressure drop across the cascade impactor and eventually a decrease in the d_{pa50} values of the lower stages (Ji et al. 2006). Therefore, dirty nozzle plates need to be cleaned regularly. For the lower 7^{th} to 10^{th} stages of the MOUDI, the nozzles may be clogged easily due to its step-shaped structure with abrupt contraction, as shown in Figures 1a-c, in which the cross sectional view, top views at the depth of 0 μm and 150 μm, respectively, are shown for the 9th stage nozzle of the MOUDI as an example (MSP Model 110). The larger dashed circle in Figure 1c shows the circumference of the step before the nozzle hole where particles may deposit easily resulting in possible nozzle clogging. In addition, since the bottom part of the nozzle used to determine the nozzle diameter is thin and fragile, cleaning by ultra-sonication is not recommended for fear that possible nozzle fracture may occur (MSP, 2006). Otherwise, ultra-sonication is an effective way to dislodge particles deposited in the nozzle.

Nozzle clogging is the other practical problem for the MOUDI. Ji et al. (2006) used an optical microscopic to observe the micro-orifice nozzles used in the each stage of the 8-stage MOUDI (MSP Model 100) after an atmospheric aerosol sampling campaign. The micro-orifice nozzles of the lower three stages were observed to be partially clogged due to particle deposition. Ji et al. (2006) further examined the effects of nozzle clogging on the performance of the impactor by evaluating the pressure drop and the particle collection efficiency for the lower three stages of the 8-stage MOUDI. They found that the pressure drops across the clogged nozzles were higher than the nominal values given by the manufacturer. The calibration results showed that the clogged nozzles had a substantial shift of collection efficiency curve to the left of the clean nozzles, and the corresponding cut-points were also decreased. That means the clogged nozzle will create errors in determining mass concentration distributions.

This study is aimed at two objectives. The first one is to determine how high the conditioned RH is needed to reduce particle bounce from different substrates to obtain accurate mass distribution and $PM_{0.1}$, $PM_{2.5}$ and PM_{10} concentrations. A humidity control system was operated upstream of two parallel MOUDIs, one of which used

silicone grease coated ALs (M1, reference MOUDI) and the other used uncoated ALs (M2) or uncoated Teflon filters (TFs, M3) as the impaction substrates. The present experimental setup enabled the study of particle bounce at different conditioned RHs (10-98%). Conditioned aerosol flow was introduced simultaneously into both MOUDIs to exclude the effect of particle loss since the same inlet was used. The second is to calibrate the particle collection efficiency curves of the 7th to 10th stages of the NMCI and those of the MOUDI ensuring the d_{pa50} values match with the nominal values given in Marple et al. (1991). After that, the total interstage loss of nanoparticles from the inlet to each lower stage (7th to 10th) of both NMCI and MOUDI was measured. The comparison test of the collocated NMCI and MOUDI was also conducted in two ambient air monitoring stations. Finally, to examine if nozzle clogging occurs in both cascade impactors, the pressure drop across the inlet to the 9th stage of the cascade impactors was monitored during sampling of incense smokes of high concentration. After the test, nozzle was examined under a microscope for possible nozzle clogging.

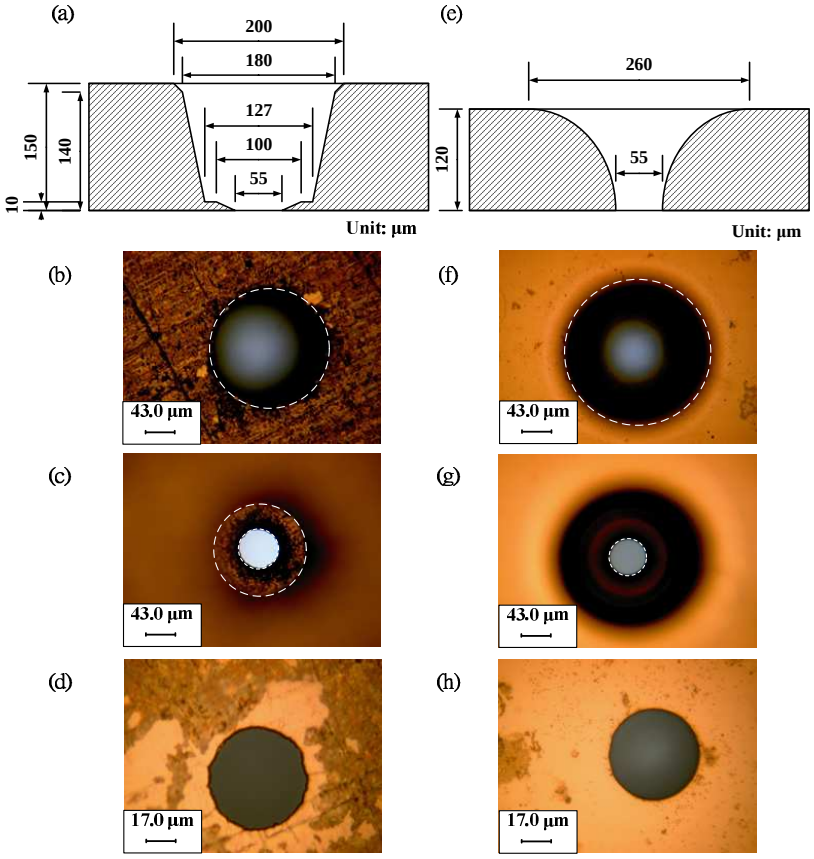

Figure 1 (a) cross-section view, front view at (b) depth=0 and (c) 150 μm, and (d) back view of a 9th stage nozzle of the MOUDI; (e) cross-section view, front view at (f)

depth=0 and (g) 120 μm, and (h) back view of a 9th stage nozzle of the NMCI. (Dashed circles demarcate the circumferences of the step or holes)

2. Method

2.1 Study of the humidity effect on the sampling performance of the MOUDI

All samplings including particle bounce tests and sampler comparisons for QC/QC of this study were conducted at a height of 15 m at the 3rd floor of the Environmental Engineering Building of National Chiao Tung University in Hsinchu, Taiwan. In total, more than forty 24-h samples were taken from January of 2009 to March of 2010 in this study.

A humidity control system consists of a humidity conditioner (FC 200-780, Perma Pure LLC, NJ, USA) with a Proportional-Integral-Differential (PID) controller, shown in Figure 2, was used upstream of two collocated MOUDIs. Fixed RHs of 10-98% at the inlet aerosol flow with variation within ±2% RH were set by adjusting the flow rates of the moist and dry sheath air of the humidity conditioner through the automatic PID controller. Normally, the set RH was stabilized within 5 min.

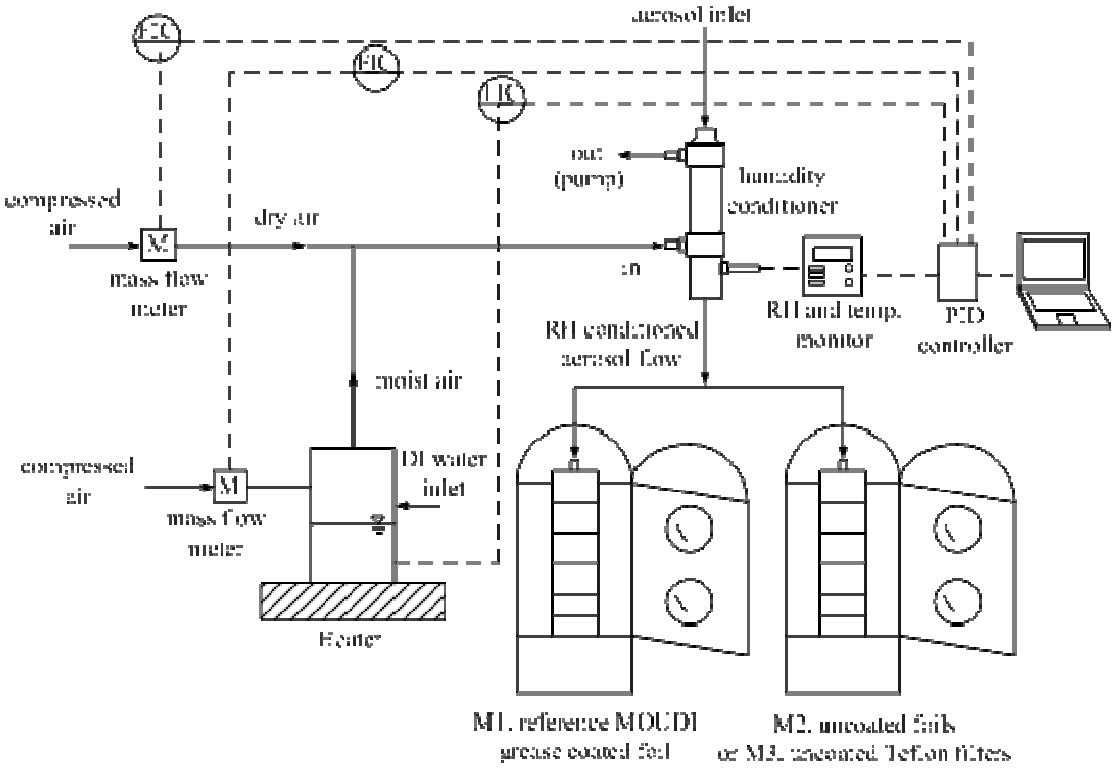

Figure 2 Schematic diagram of the present experimental system.

In the MOUDIs, the nozzle plates of 3.2 μm cutsize were replaced with those of 2.5 μm cutsize and the 56 nm cutsize nozzle plates (stage 10) was removed so that

only $PM_{0.1}$ was collected by the after filter. That is, the cutsizes of the MOUDIs in this study were 18, 10, 5.6, 2.5, 1.8, 1.0, 0.56, 0.32, 0.18 and 0.1 μm at sampling flow rate of 30 L/min. Teflon filters (TefloR2PL037, Pall Corp., New York, US) were used at the after filter stage of each of every tested MOUDIs while three different impaction substrates were used in stage 0-9 of three different MOUDIs, respectively, including grease coated ALs (M1), uncoated ALs (M2) and uncoated TFs (M3, TefloR2PL047, Pall Corp., New York, US). Conditioned aerosol flow was simultaneously introduced into M1 and M2 or M1 and M3, respectively, and the effect of particle bounce on PM measurement was determined by comparing the PM mass concentration collected on every stage of the MOUDIs as:

$$\frac{\left|\left(C_{iM1}-C_{iM2}\right)\right|}{C_{iM1}} \text{ or } \frac{\left|\left(C_{iM1}-C_{iM3}\right)\right|}{C_{iM1}} \quad (1)$$

where $C_{i\ M1}$, $C_{i\ M2}$ and $C_{i\ M3}$ are the PM mass concentrations at stage i of M1, M2 and M3, respectively (i=0-9 for impaction stages, i=10 for after filter stage). The effect of particle bounce on $PM_{2.5}$ and PM_{10} concentrations was also examined, when $PM_{2.5}$ and PM_{10} were calculated as the sum of PM mass concentrations from i=4 to i=10 (or after filter) and i=2 to i=10, respectively, and also based on the collection efficiency curve of EPA $PM_{2.5}$ Well Impactor Ninety-Six (Peters et al., 2001) and Hi-Vol Sampler (McFarland et al., 1984), respectively.

The M1 was regarded as the reference MOUDI since it was comparable with a collocated SMPS (Model 3936, TSI Inc., MN, USA) for $PM_{0.32}$, $PM_{0.18}$ and $PM_{0.1}$, illustrating particle bounce was significantly eliminated of M1 by the use of grease coated substrate in the MOUDI of this study. In our previous study, MOUDI M1 using the uncoated ALs and the Teflon after filter was applied to obtain the chemical mass closure of $PM_{0.1}$ at different atmospheric environments successfully (Chen et al., 2010a; b). The $PM_{0.1}$ concentration measured by M1 was found to agree with that converted from the number concentration of a SMPS by using the effective density obtained by Chen et al. (2010a). Besides, the $PM_{2.5}$ and PM_{10} concentrations of M1 were also found to be in very good agreement with those of a collocated Dichotomous sampler (Model SA-241, Andersen Inc., Georgia, USA) with an average relative difference of less than 6.3±1.7% (average ± standard deviation).

Before particle bounce test, three MOUDIs (M1, M2 and M3), all of which used grease coated AL substrates in stages 0-9 and TF in the after filter were collocated to compare the mass distributions of atmospheric aerosols to ensure no bias between them. Totally five 24-h measurements were conducted. In addition, two MOUDIs

(M1 and M2), one of which with and the other without installing the humidity conditioner at its inlet, were compared for PM concentration in the field to examine particle loss in the humidity conditioner. Five 24-h measurements were conducted during the days of high atmospheric RHs of 80-95% (cloudy and rainy day) when particle bounce did not occur (Vasiliou et al., 1999). Loss of submicron and ultrafine particles with diameter smaller than 0.6 μm in the humidity conditioner was examined more clearly by introducing polydisperse NaCl particles, which were produced by atomizing NaCl solution using an atomizer (Model 3076, TSI Inc., MN, USA), into the humidity conditioner. Subsequently, the loss was determined by comparing the size distributions of NaCl particles at the humidity conditioner upstream and downstream.

In every sampling run, at least two TFs and two uncoated and silicone grease coated ALs (or >10% of sample number) were used as laboratory and field blanks, respectively, for gravimetric analysis. All filter samples were conditioned at least for 24-h in a temperature and relative humidity controlled room (21.5±1 ^{o}C, 40±5% RH) before and after sampling. For coated ALs, 0.3 to 0.5 mg of Silicone grease (KF-96-SP, Topco Technologies Corp., Taiwan) was applied uniformly on the foils (Chen et al., 2010b; Pak et al., 1992). After coating, the foils were baked in an oven at 65 ^{o}C for 90 min (Marple et al., 1991). The electrostatic charge of the TFs was eliminated by an ionizing air blower (Model CSD-0911, MEISEI, Japan) before weighing. A microbalance (Model CP2P-F, Sartorius, Germany) was used to weigh the filters after they were conditioned for at least 24-h in the temperature and relative humidity controlled room (21.5±1 ^{o}C, 40±5% RH) before and after samplings.

The possibility that the coated silicone grease might evaporate from stages 0-9 during sampling and absorbed by the collected $PM_{0.1}$ or the after filter was examined before the sampling campaign. The weight of the coated ALs before sampling and the weight of the ALs after sampling cleaning air for 24-h, when two HEPA capsules were installed at the MOUDI inlet, were compared to check if the evaporation occurred from the coated ALs. Results showed that the weight difference was <2 μg for each foil of stages 0-9, indicating evaporation was negligible during sampling. That is, use of silicon grease in stages 0-9 did not interfere with the mass of $PM_{0.1}$ in this study.

2.2 Measurement of collection efficiency and interstage loss in the MOUDI and NMCI.

The experimental setup for measuring particle collection efficiency and nanoparticles loss is shown in Figure 3. Monodisperse liquid dioctyl sebacate (DOS) particles with the aerodynamic diameter (d_{pa}) from 15 to 500 nm were generated by

the atomization and electrostatic classifier technique for the test. Polydisperse particles were first generated by the constant output atomizer (TSI Model 3076) from the DOS solution with the concentration from 0.001 to 0.1 % (v/v). The aerosol flow was passed through a tubular furnace at a fixed temperature of 300 ^{0}C to produce a relatively narrow size distribution by the evaporation-condensation process. Monodisperse, singly charged particles were then generated by the electrostatic classifier (EC, TSI Model 3080) equipped with the nano-differential mobility analyzer (DMA, TSI Model 3085) or the long-DMA (TSI Model 3081). To minimize the effect of multiple charges on the monodispersity of the classified particles (Pui and Liu, 1979), only particles larger than the count median diameter (CMD) were classified. When calibrating the particle collection efficiency of a single lower stage, a ball valve was used to simulate the pressure drop created by all previous upstream stages. The following equation was then used to calculate the particle collection efficiency (η) or interstage loss (L) as:

$$\eta \text{ or } L = \left(1 - \frac{I_2}{I_1}\right) \times 100 \tag{1}$$

where the I_1 and I_2 are the aerosol currents at the inlet or outlet of the tested impactors measured by the TSI 3068 aerosol electrometer (AE) equipped with a home-made faraday gage which is similar to that used in the AE but has a larger flow passage inside to reduce the pressure drop.

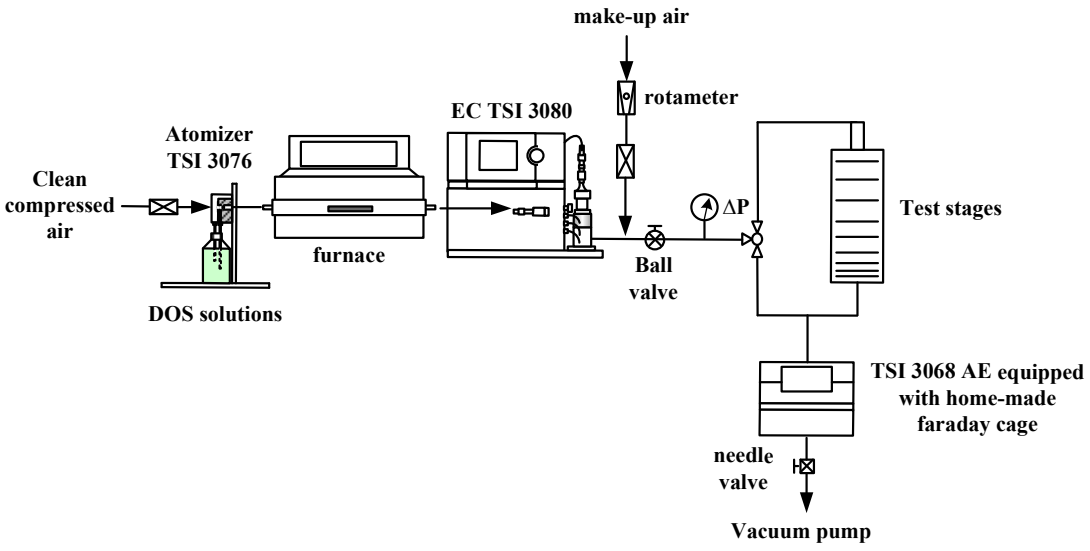

Figure 3 Experimental setup to measure the particle collection efficiency and nanoparticle loss.

2.3 Field comparison and nozzle clogging test

After the laboratory tests, field comparison and nozzle clogging tests were conducted. For the field comparison test, the NMCI and the MOUDI were collocated to measure ambient aerosol mass size distributions at the Jhong-Shan and Jhu-Dong air monitoring stations, Taiwan. Silicone grease (KF-96-SP, Topco Technologies Corp., Taiwan) coated aluminium foils were used as the impaction substrates in the 0^{th} to 10^{th} stages to reduce solid particle bounce, and Teflon filters (Zefluor P5PJ047, Pall Corp., New York, USA) were used as the after filter. Before weighing, the substrates were conditioned in an environmental conditioning room where the RH and temperature were kept at 40 ± 2 % and 21 ± 1 ℃, respectively. A microbalance (Model CP2P-F, Sartorius, Germany) was used for weighing, in which the electrostatic charge of the Teflon filters were neutralized by an ionizing air blower (Model CSD-0911, MEISEI, Japan).

To examine possible nozzle clogging, the pressure drop of the NMCI and the MOUDI was monitored continuously during sampling of high concentration (25 mg/m^3) incense smokes with the mass median aerodynamic diameter (MMAD) of 500 nm for 45 min. After sampling, dirty nozzle plates were observed under an optical microscopy (ESPA, Model IM35) for possible nozzle clogging.

3. Results and discussion

3.1 QA/QC results

The gravimetric analysis of all laboratory and field blanks showed that weight differences between pre- and post-sampling were less than 3 μg, which was a relatively low value compared to the typical weight of 43 μg for the typical $PM_{0.1}$ concentration of 1 $\mu g/m^3$ in urban areas. The comparison of mass concentrations of ambient particles between three collocated MOUDIs showed a very good agreement for all size intervals, especially for the last three stages ($PM_{0.18-0.32}$, $PM_{0.1-0.18}$ and $PM_{0.1}$) as shown in Figure 4. Other five repeated tests conducted at different days showed similar results. Particles at the present site were seen to be bimodal including the accumulation and coarse modes, which enabled the investigation the bounce of UFPs, fine and coarse particles at the same time for different impaction substrates at different RHs.

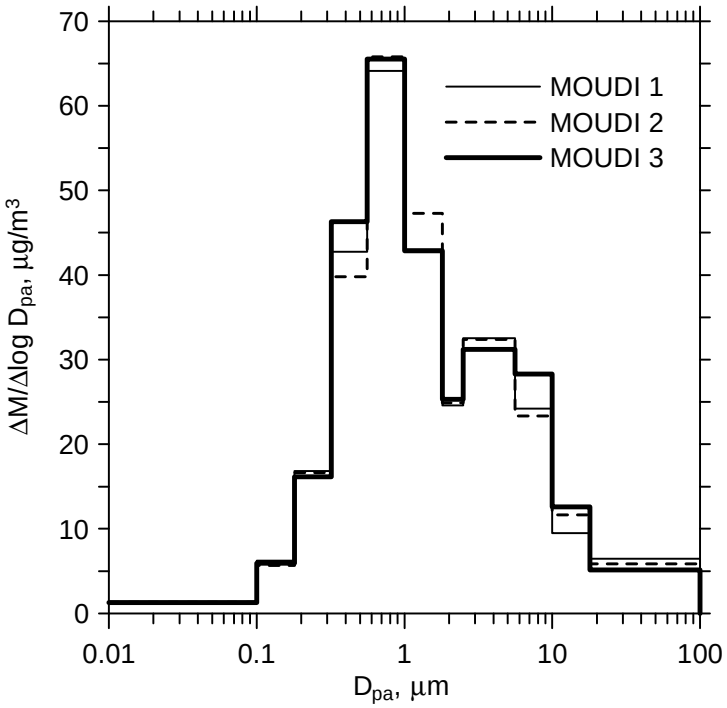

Figure 4 Comparison of particle mass distributions between three collocated MOUDIs.

3.2 Particle loss in the humidity conditioner

Figure 5 shows the comparison of mass distributions between the MOUDI with the humidity conditioner installed and that without. There was no control of the RH for the MOUDI with humidity conditioner and both MOUDIs sampled aerosols at RHs of 80-95%. The MMADs of the accumulation and coarse particle modes of the MOUDI with the conditioner were found to be 3.56 and 0.45, respectively, while those without were 3.95 and 0.45 μm, respectively. Similar accumulation mode MMADs and mass concentrations in each stage below the 2.5 μm cutsize stage between the two MOUDIs indicated that particles loss in the humidity conditioner was low for fine particles. However, a smaller coarse mode MMAD (with difference of ~10%) and a lower mass concentrations in each stage above the 2.5 μm stage of the MOUDI with the conditioner than that without was found, indicating loss of coarse particles occurred in the humidity conditioner. Loss of $>PM_{18}$ (stage 0), $PM_{10\text{-}18}$ (stage 1), $PM_{5.6\text{-}10}$ (stage 2) and $PM_{2.5\text{-}5.6}$ (stage 3) was 72.5, 52.3, 20.9 and 5.3%, respectively, in the conditioner leading to the underestimation of these large particles. $PM_{0.1}$ concentrations of the two collocated MOUDIs, which were 0.56 and 0.53 $\mu g/m^3$, respectively, were in very good agreement with a difference of only 5.4%. Other five repeated measurements showed similar results.

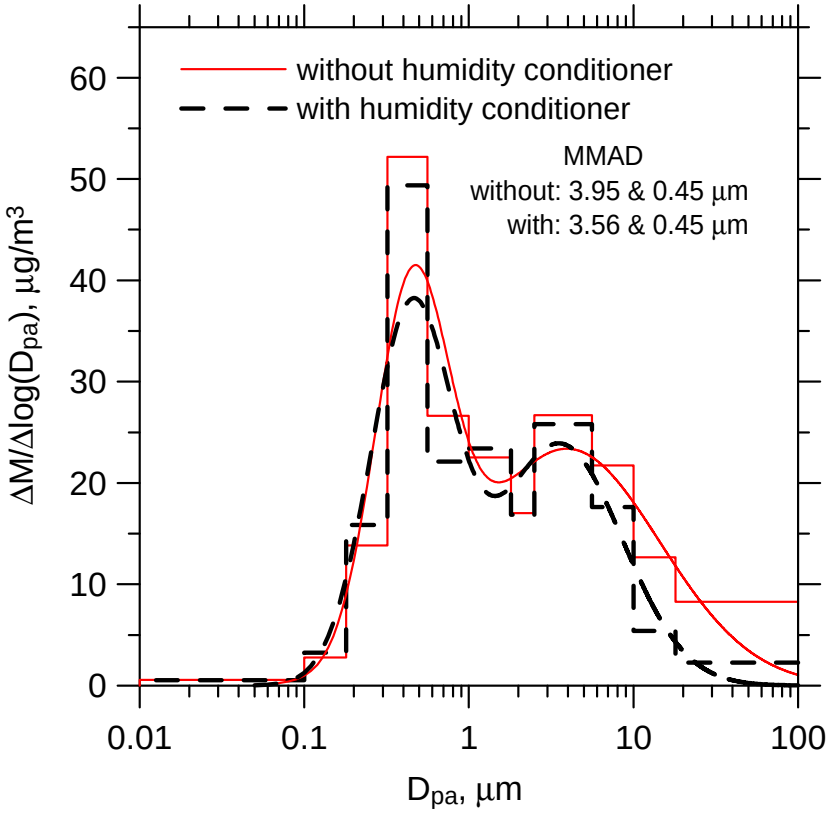

Figure 5 Comparison of particle mass distributions between two collocated MOUDIs with and without installing humidity conditioner, ambient RH=80-95%. Note: There was no control of the RH for the inlet aerosols for the MOUDI with the humidity conditioner.

For the humidity conditioner, Figure 6 compares the experimental data of particle loss for particles smaller than 0.6 µm in aerodynamic diameter with the theoretical values based on the equation of Gormley and Kennedy (1949). In the figure, the aerodynamic diameter of NaCl was converted from the mobility diameter of SMPS assuming the NaCl density of 2.2 g/cm^3. As can be seen in the figure, the experimental particle loss was in very good agreement with the predicted value by a maximum difference of ~4%. The experimental loss increased from 3.4 to 20.3% as particle diameter was decreased from 100 to 15 nm. Slightly higher experimental loss than the prediction for particles larger than 100 nm was due to the effect of inertial impaction and gravity which was not considered. From the particle loss data, it was calculated that the loss of $PM_{0.1}$ mass in the conditioner was only ~5%, which was almost the same as that determined by the gravimetric method as shown in Figure 5. In summary, installing the humidity conditioner at the MOUDI does not lead to fine and nanosize particle loss, while particle loss for coarse particles is severe.

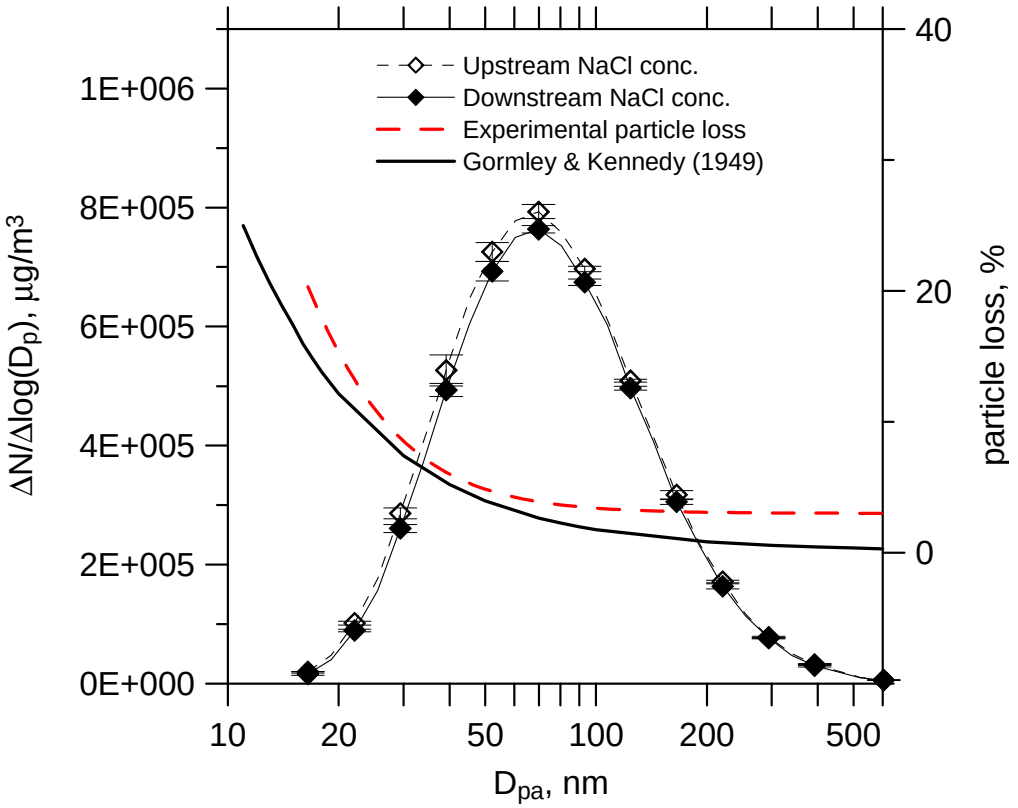

Figure 6 Comparison of particle loss in the humidity conditioner for particles smaller than 0.6 μm between the experimental data and calculated by the equation of Gormley and Kennedy (1949).

3.3 Particle bounce effect on mass distribution

Figure 7 compares the mass distributions and fitted MMADs of M1 with those of M2 and M3 at 25, 50 and 75% of RH. The data shown here for these RHs was because they covered dry, moderate and wet conditions of aerosols when particle bounce can be observed and quantified simply. Again, the substrates in M1, M2 and M3 were greased coated ALs, uncoated ALs and uncoated TFs, respectively. Both accumulation and coarse MMADs of M2 and M3 were in good agreement with those of M1 at 50 and 75% RHs as shown in Figures 7 (c-f). Consistent agreement was found for the accumulation MMAD as RH reduced to 25% (Figures 7 (a) and (b)). However, discrepancy of the coarse MMAD occurred between coated M1 and uncoated M2 and M3 at this decreased RH, meanwhile mass distribution of M2 and M3 was observed to shift toward smaller diameters obviously compared with M1. A more severe of shifting toward the left was found at RH < 25% for both M2 and M3 (data was not shown).

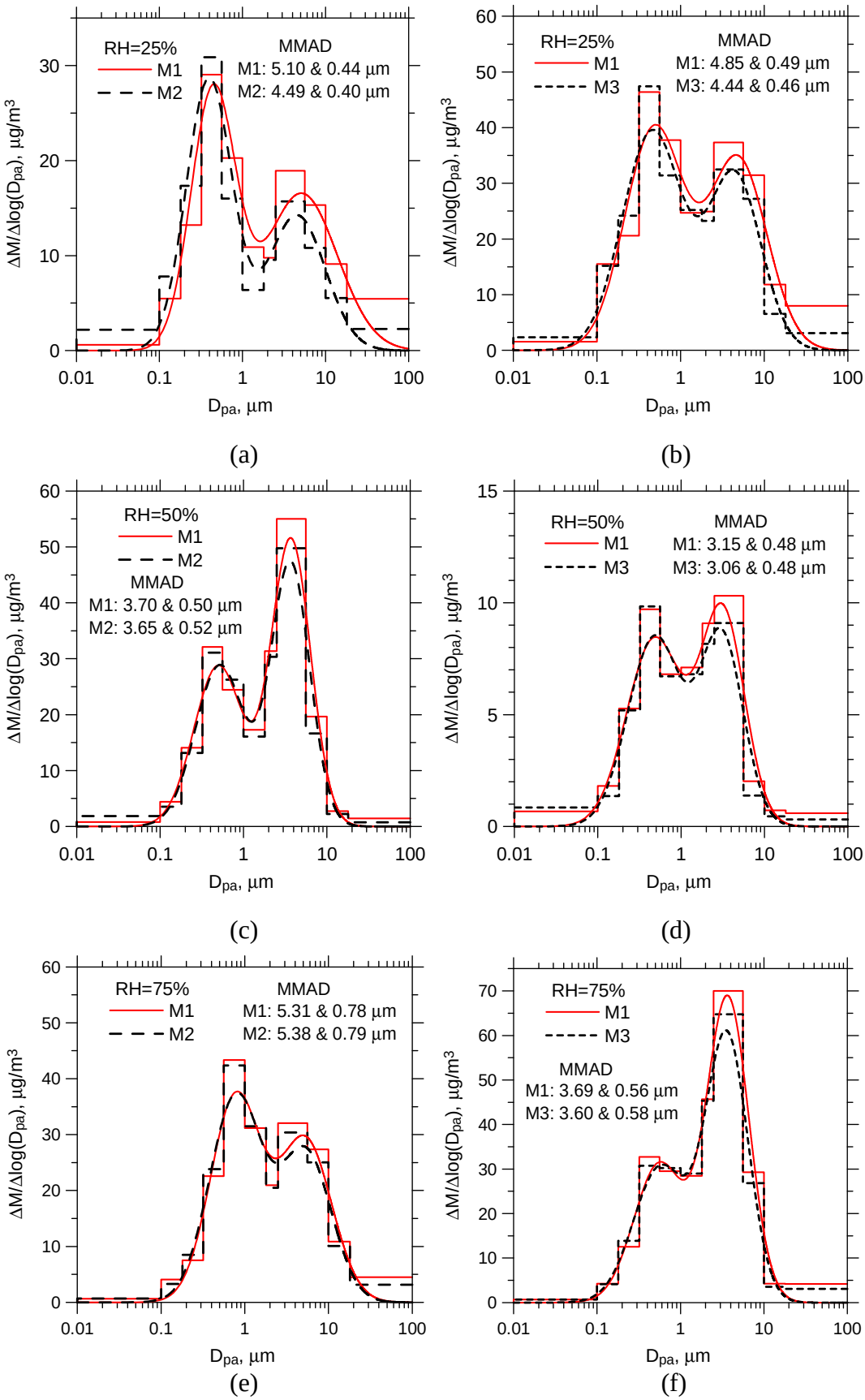

Figure 7 Comparison of particle mass distributions and MMADs of M2 or M3 to those of M1 at conditioned RHs of 25, 50 and 75%.

Comparing the collected PM mass of M1 with those of M2 and M3, it was found that M1 sampled more $PM_{2.5-10}$ mass (sum of stages 2 and 3) than M2 and M3 significantly at both RHs of 25 and 50%. M2 was more different from M1 than M3 as the RH was same. M2 and M3 undersampled $PM_{2.5-10}$ by 22.5 and 14.2% at RHs of 50%, respectively, while those at 25% RH were 11.0 and 10.2%. Besides, M2 and M3 were also found to undersample $PM_{2.5-10}$ even at the RH as high as ~75% (Figures 7 (e-f)) when the differences were both reduced to below 7%. The difference was found to reduce further at RH of 80-98% when it was < ~3% (data was not shown). Since the undersampling of $PM_{2.5-10}$ reduced with increasing RH, it could be attributed to the occurrence of particle bounce in M2 and M3 at RH < 75%. The finding of particle bounce for particles larger than 2.5 μm was in agreement with that has been observed by Dzubay et al. (1976). Note that more accurate sample of coarse particle ($PM_{2.5-10}$) could be collected only when RH was increased to ~80% once uncoated MOUDI was used. Importantly, the bouncing particles were found to get loss on the inner wall of MOUDI rather than jump to lower stages because PM mass did not increase correspondingly at stages after the stage of 2.5 μm cut. This was also demonstrated by the observation that particles deposited on the inner wall in stages 0-3 of MOUDI.

The average $PM_{0.1}$ determined by M1 for the total forty samples was 0.8±0.3 $\mu g/m^3$ (average ± standard deviation), which was comparable to the average concentration at the urban areas in LA obtained by Cass et al. (2000). As was mentioned previously, the present M1 sampled a close $PM_{0.1}$ to the collocated SMPS. These indicate that the present M1 can be used to determine the overestimation of $PM_{0.1}$ by M2 and M3 as bounce occurred.

It was found M2 and M3 both collected very close $PM_{0.1}$ to M1 at RH of 75% as shown in Figures 7 (e) and (f). However, it was observed that bouncing particles from front stages (normally stages 9 and 8) contributed to $PM_{0.1}$ sample with a significant amount of >30% (shown more detailed later) at RHs of 25 and 50% as seen in Figure. 7 (a-d). The quantity of $PM_{0.1}$ oversampling at 25% RH was very close to that shown in Figure 9 of Vasiliou et al. (1999). Note that, accurate $PM_{0.1}$ sample can be obtained as RH is high enough, typically >75% RH, even uncoated substrates are used in the MOUDI but significant error on $PM_{0.1}$ concentration exists at low RH (<50%) once bounce occurs. Particles could also bounce from middle stages (4-6 stages) and be collected at lower stages (7-after filter) at RH of 25% when uncoated ALs were used as shown in Figures 7 (a) and (b). In addition, more severe bounce in M2 than M3 at the same RH (25 or 50%) for $PM_{0.1}$ was found, which could be due to more rigid surface of uncoated ALs than TFs.

Accumulation mode particles include products of combustion processes and are considered on a mass basis to be more toxic because they contain hazardous materials

and more readily reach the respiratory region (Oberdörster et al., 2005). In order to completely know the level of distortion of the accumulation mode in wide-ranging RHs, the ratio of accumulation MMADs of M2 and M3 to M1 at RHs from 10 to 98% was compared in Figure 8. As is seen, the MMADs of M2 and M3 were both in good agreement with M1 at RH > ~40% when the difference was within ±5%. However, difference increased with decreasing RH and the ratio was decreased to ~0.75 and ~0.9 for M2 at RH of 10% and M3 at RH of 20%, respectively. That is, accumulation mode particles can be collected accurately by MOUDI as RH >40% even uncoated substrates are used.

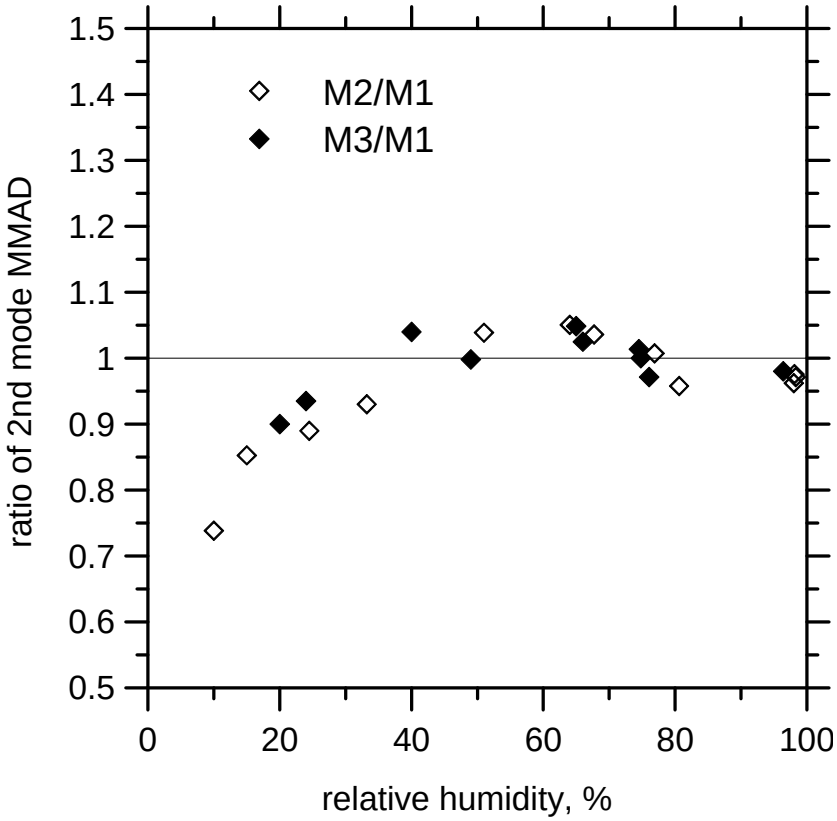

Figure 8 Ratio of accumulation mode MMADs of M2 or M3 to those of M1 at different conditioned RHs.

3.4 PM ratios of M2 and M3 to M1

As discussed previously, particle bounce in the MOUDI can lead to oversampling of $PM_{0.1}$, the loss of coarse particle on the inner wall and shifting of size distribution toward the smaller diameter. All these may result in sampling errors of $PM_{0.1}$, $PM_{2.5}$ and PM_{10} by the MOUDI. PMs ratios of M2 and M3 to M1 at different RHs are compared in Figure 9 to examine the effect of RH changes and different impaction substrates on particle bounce. The linear regressions of $PM_{0.1}$ and PM_{10} ratios are also shown in the figure. Note that the regression line of PM_{10} was fitted

from pooling both data of M2 and M3 since they showed a similar trend. From the figure, it is observed that ratios of M2 and M3 to M1 are close to 1 for all PMs at high RHs of 75-98%. Surprisingly, the $PM_{2.5}$ ratios of M2 and M3 were both found to be near 1 even when RH decreased from 75 to 10 % or to 20%, respectively. However, PM_{10} ratios were decreased to ~0.75 and ~0.8 for M2 and M3, respectively at these low RHs. This was due to particle loss of coarse particle ($PM_{2.5-10}$) at the reduced RH as discussed previously. Although M2 and M3 sampled a close $PM_{2.5}$ to M1 even at low RH of 10 or 20%, their mass distribution and accumulation MMADs deviated from those of M1 as shown in Figures 7(a-b) and Figure 8, respectively. This is because bouncing fine particles contributed to the following stage samples rather than lost in the MOUDI inner wall as coarse particles.

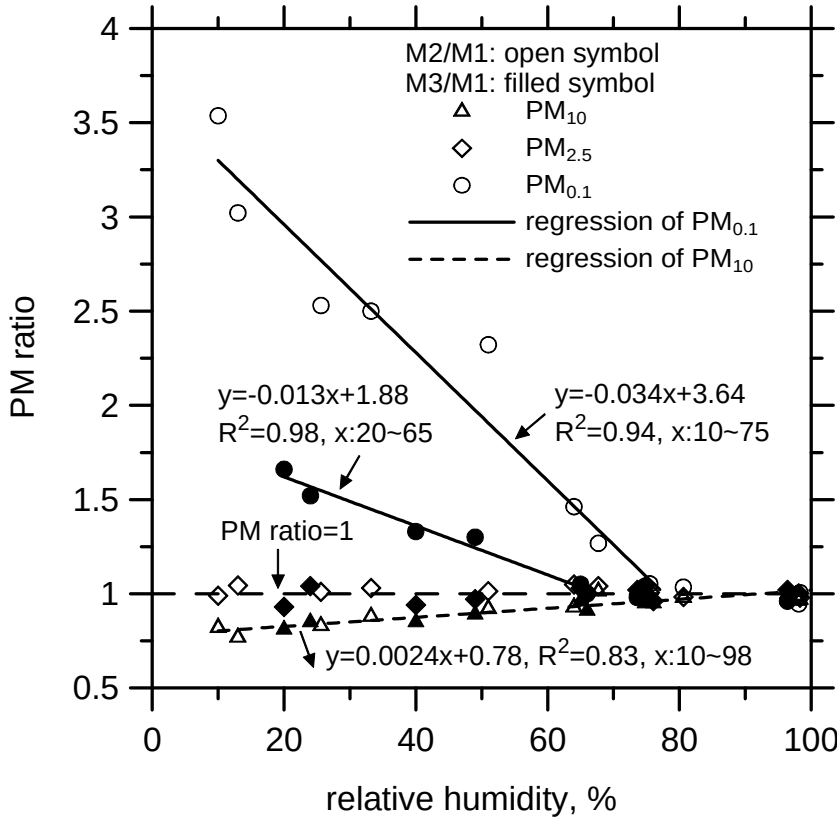

Figure 8. PM_{10}, $PM_{2.5}$ and $PM_{0.1}$ ratio of M2 or M3 to M1 at different conditioned RHs.

Particle bounce, leading to the oversampling of $PM_{0.1}$ was illustrated in this study. The quantity of $PM_{0.1}$ oversampling for both M2 and M3 increased with decreasing RH, where M2 was more severe than M3 at the same RH. This was because Teflon filter has fibrous porous structure and fine particles can easily get impacted and filtered by the substrate with less particle bounce and blowing off. As a result, uncoated TF MOUDI samples much less $PM_{0.1}$ in the after filter as compared

to uncoated AL MOUDI. Based on the data and linear regression, it was found bounce occurs in M2 and M3 and they started to oversample $PM_{0.1}$ at RHs below 75 and 65%, respectively, which was in agreement with those found by Stein et al. (1994) and Vasiliou et al. (1999). M2 oversampled $PM_{0.1}$ mass by 95 and 180% at RH of 50 and 25%, respectively, while those of M3 were 25 and 55%. Based on the present results and Fang et al. (1991) in which flow-induced humidity changes on size cut was examined, it is concluded accurate $PM_{2.5}$ and $PM_{0.1}$ can be obtained with less than 5 % of error at RHs of 65-80% and 75-80% when uncoated ATs and uncoated ALs are used as the impaction substrates of MOUDI, respectively. This can be achieved by using the present humidity control system since it can control RH from 5 – 98 % stably with a deviation of only ±2% RH and a negligible loss for fine particles and UFPs.

3.5 Particle collection efficiency curves of the NMCI and the MOUDI

Figure 10 shows the calibrated particle collection efficiency curves of the 7^{th} to 10^{th} stage of the NMCI and those of the MOUDI. The calibration results together with the design parameters are summarized in Table 1. It shows that after adjusting proper S/W ratios (S: jet to plate distance; W: nozzle diameter), the d_{pa50} values of the 7^{th} to 10^{th} stage of the NMCI and those of the MOUDI are close to the nominal values, which are 320, 180, 100 and 56 nm, respectively, given in Marple et al. (1991). The S/W ratio of the 9^{th} stage of the NMCI, 13.44, is very close to that of the micro-orifice impactor in the PENS (personal nanoparticle sampler) in which d_{pa50} is 100 nm and S/W is 13.8 (Tsai et al. 2012).

From Table 1, it can also be seen that the S/W ratios of the 7^{th} and 8^{th} MOUDI stages, which are 5.56 and 11.32, respectively, are larger than those of the NMCI, which are 2.52 and 3.01, respectively. This is because that the nozzle diameters of the former are smaller than the latter. Conversely, the S/W ratios of the 9^{th} and 10^{th} MOUDI stages, which are 9.3 and 10.9, respectively, are smaller than those of the NMCI, which are 13.44 and 24.75, respectively, because the corresponding nozzle diameters of the former are larger than the latter. Besides the difference in the nozzle diameter, partial particle clogging in the 7^{th} and 8^{th} stages of the MOUDI after it has been used for more than 5 years despite its regular nozzle cleaning may also explain why different S/W ratios are needed to maintain the correct d_{pa50} values. Smaller nozzle diameter in the 10^{th} NMCI stage also leads to a larger pressure drop and a larger S/W ratio is needed to maintain the d_{pa50} of 56 nm as compared to the MOUDI. Similar sensitive S/W effect on the cutoff diameters was also found in the PENS (Tsai et al. 2012), which deserves future study to facilitate the design of the micro-orifice cascade impactor.

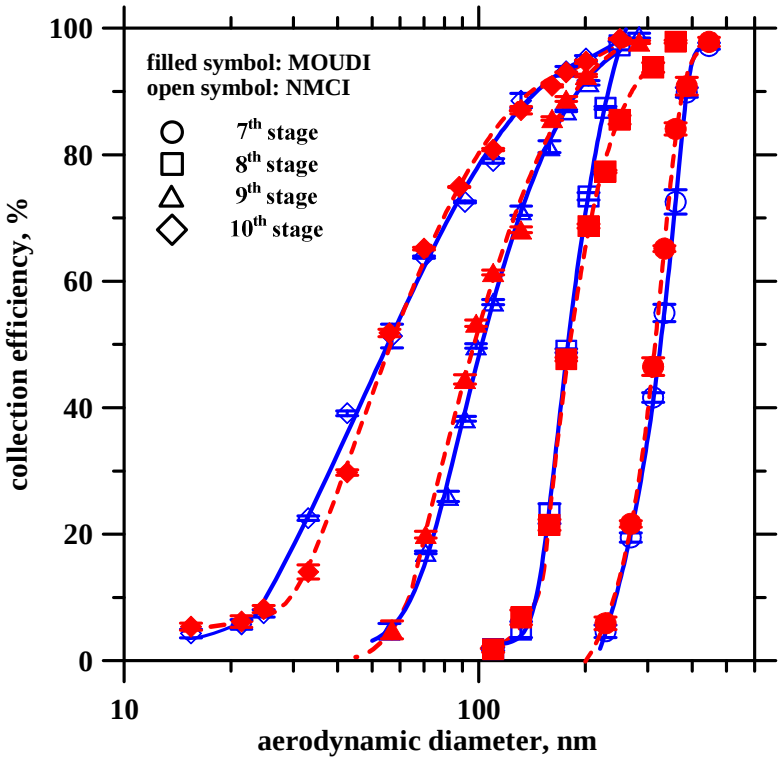

Figure 10 Particle collection efficiency curves of the 7th to 10th stages of the MOUDI and NMCI.

Table 1 Summary of the calibration results and the design parameters of the 7th to 10th stage of the NMCI and the MOUDI.

Stage	Marple et al. (1991)				MOUDI				NMCI			
	Nominal d_{pa50} (nm)	Nozzle dia. (μm)	[a]S/W	[b]P/P$_0$	d_{pa50} (nm)	Nozzle dia. (μm)	[a]S/W	[b]P/P$_0$	d_{pa50} (nm)	Nozzle dia. (μm)	[a]S/W	[b]P/P$_0$
7	320	140	4.1	0.95	314.4	135	5.56	0.95	323	138.7	2.52	0.95
8	180	90	6.4	0.89	180.8	102	11.18	0.87	178.5	109.5	3.01	0.89
9	100	55	10.6	0.76	97.0	57	9.30	0.72	102	54.3	13.44	0.72
10	56	52	11.1	0.53	56.5	52.3	10.90	0.47	55.7	50.9	24.75	0.34

[a] S=jet to plate distance, W=nozzle diameter.

[b] P=absolute pressure at stage exit with all upstream stages in place, P$_0$=ambient pressure.

The above calibration results are for the individual stages of the two cascade impactors. When the upstream stages are present, the total collection efficiency curves form the inlet to one of the lower stages is shown in Figure 11. The left tail ends of the total collection efficiency curves are seen to lift upward when the upstream stages are present due to the convectional diffusion of nanoparticles in the stages. Similar results were also found in previous studies (Marple et al. 1991; Tsai et al. 2012). It can also

be observed that for the inlet to the 9th or 10th stage, there is a shift of the collection efficiency curve to the left (i.e. to the smaller particle size) as compared to that calibrated individually, and the corresponding d_{pa50} is decreased from 102 to 92.4 nm or 55.7 to 47.1 nm, respectively.

An additional check was also made by estimating the total collection efficiency from the inlet to the 9th stage ($\eta^*_{T,9}$) or to the 10th stage ($\eta^*_{T,10}$) using the following equation:

$$\eta^*_{T,i} = 1-(1-\eta_{T,i-1})(1-\eta_i) \quad (2)$$

where $\eta_{T,i}$ and η_i are the total collection efficiency of the inlet to the i^{th} stage and the collection efficiency of the individual i^{th} stage, respectively. Results are plotted as filled symbols in Figure 11 in which $\eta^*_{T,10}$ and $\eta^*_{T,9}$ are shown to agree well with those of the experimental total collection efficiencies with the average absolute relative difference of 3.2 and 4.2 %, respectively. For the 8th stage, however, such a shift in the collection efficiency curve is not observed. This is because that partial overlapping of the lower part of the collection efficiency curve of the 8th or 9th stage with the upper part of the collection curve of the 9th or 10th stage occurs. In addition, the total collection efficiency curves of the inlet to the 9th and 10th stage are affected by convectional diffusion deposition of nanoparticles in all previous stages, which is only important for nanoparticles, or particles with d_{pa} less than 100 nm. Therefore, in order to obtain more accurate size resolution of nanoparticles, nanoparticle loss of all upstream stages should also be considered.

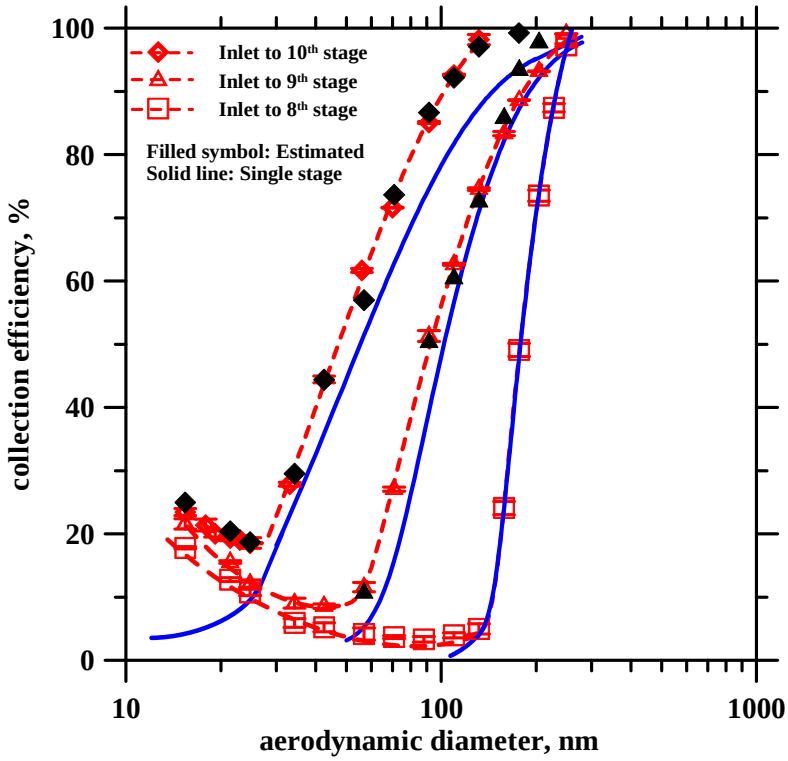

Figure 11 Particle collection efficiency curves of the 8th to 10th stage of the NMCI with all upstream stages in place.

3.6 Interstage loss of nanoparticles in the NMCI and the MOUDI

Figure 12 shows the total interstage loss of nanoparticles from the inlet to each of the lower stages of the NMCI and those of the MOUDI. It is noted that in order to distinguish the interstage loss of nanoparticles from the collection efficiency of the 9th and 10th stages, only particles with d_{pa} near the lower end of the collection efficiency curve where $d_{pa} < d_{pa50}$ were used for the tests, which were 15.4 to 42.5 and 15.4 to 25 nm, respectively. For other stages, nanoparticles with d_{pa} from 15.4 to 105 nm were used. Results show that total nanoparticle loss increases with decreasing d_{pa} due to convectional diffusion deposition. The maximum loss from the inlet to the 6th to 10th stage occurs at d_{pa} of 15.4 nm, which is 11.39 to 23.47 % for the NMCI, and 12.83 to 26.13 % for the MOUDI. The total interstage loss of nanoparticles in the NMCI is slightly lower than those in the MOUDI due to smoother nozzle shape of the former. For both impactors, a significant total interstage loss of nanoparticles from the inlet to one of the lower stages (7th to 10th) exists especially for nanoparticles with the diameter smaller than 40 nm. For nanoparticles larger than 40 nm, the total interstage loss is less than 10 % and it decreases with increasing particle diameter. It is therefore important to consider the nanoparticle loss in the 10th stage when determining the mass distributions of nanoparticles.

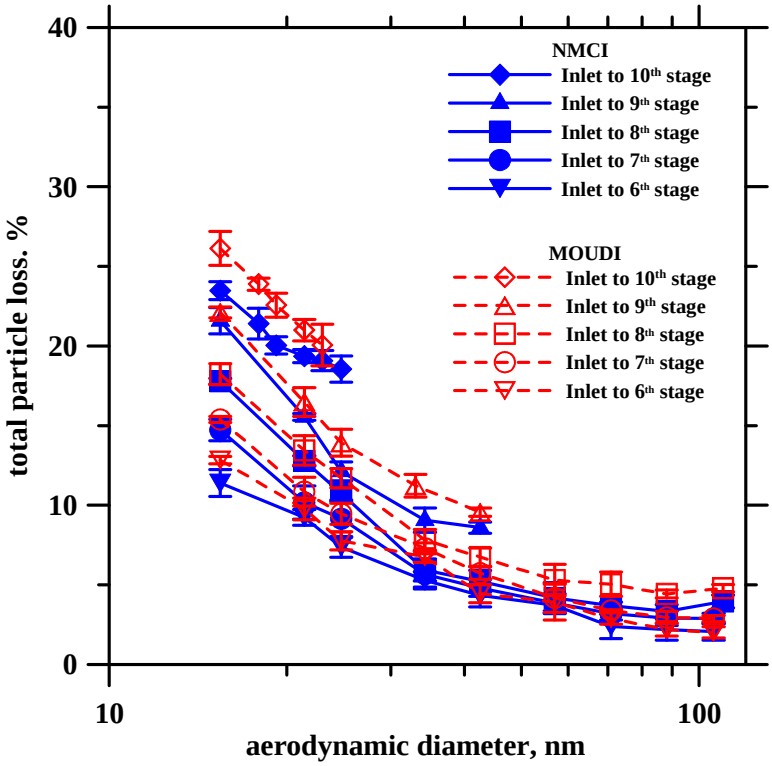

Figure 12 Total interstage loss of nanoparticles from the inlet to different stages of the MOUDI and NMCI.

In order to determine how much loss exists in each single stage, the following equation is used:

$$L_i^* = \frac{L_{T,i} - L_{T,i-1}}{1 - L_{T,i-1}} \tag{3}$$

where L_i^* is the estimated single stage loss in the i^{th} stage, and $L_{T,\,i}$ is the experimental total interstage loss from inlet to the i^{th} stage. The L_7^* to L_9^* of the NMCI and those of the MOUDI are shown in Figure 13 where it shows the loss is below 5 % for each single stage and is gradually increased with decreasing d_{pa} due to convectional diffusion deposition. This small particle loss per individual stage prevents accurate loss measurement as stated in the previous section. The maximum L_7^* to L_9^* occur at d_{pa} of 15.4 nm, which are 3.59 to 4.61 % and 2.93 to 4.74 %, for the NMCI and the MOUDI, respectively. The loss L_0^* to L_6^* is estimated to be small,

which is less than 1.6 and 1.8 %, if the total loss $L_{T,6}$ of 11.39 and 12.83 % is assumed to be evenly divided in the inlet to 6th stages for the NMCI and the MOUDI, respectively.

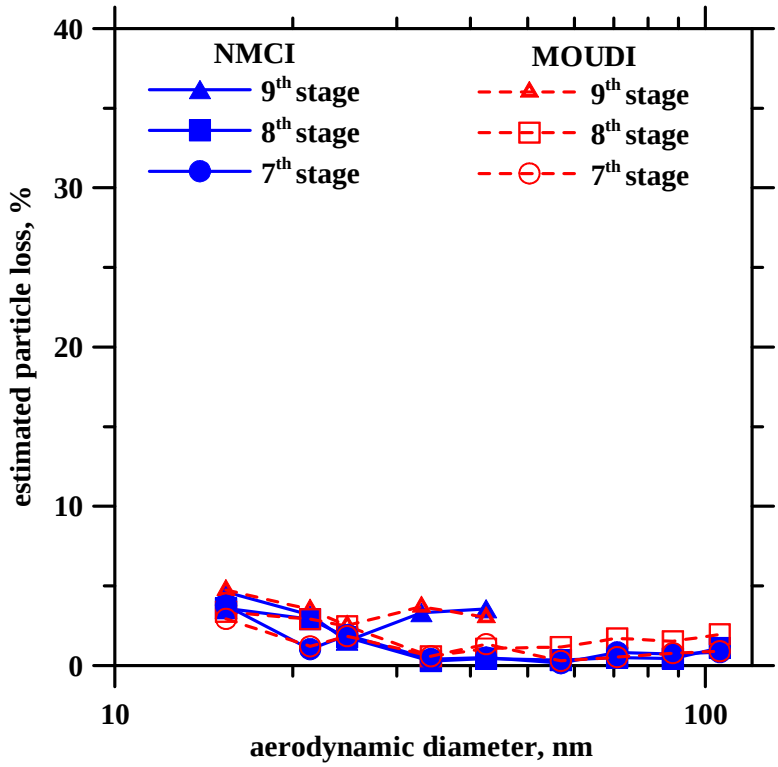

Figure 13 Estimated single stage nanoparticle loss in the 7 to 9th stage of the MOUDI and NMCI.

3.7 Field comparison and nozzle clogging test

The ambient mass size distributions measured by the NMCI and those by the collocated MOUDI are shown in Figure 14. The mass size distributions measured by the NMCI are seen to be very close to those by the MOUDI. Most of the data between the stages of these two cascade impactors have the relative difference of less than 10 %.

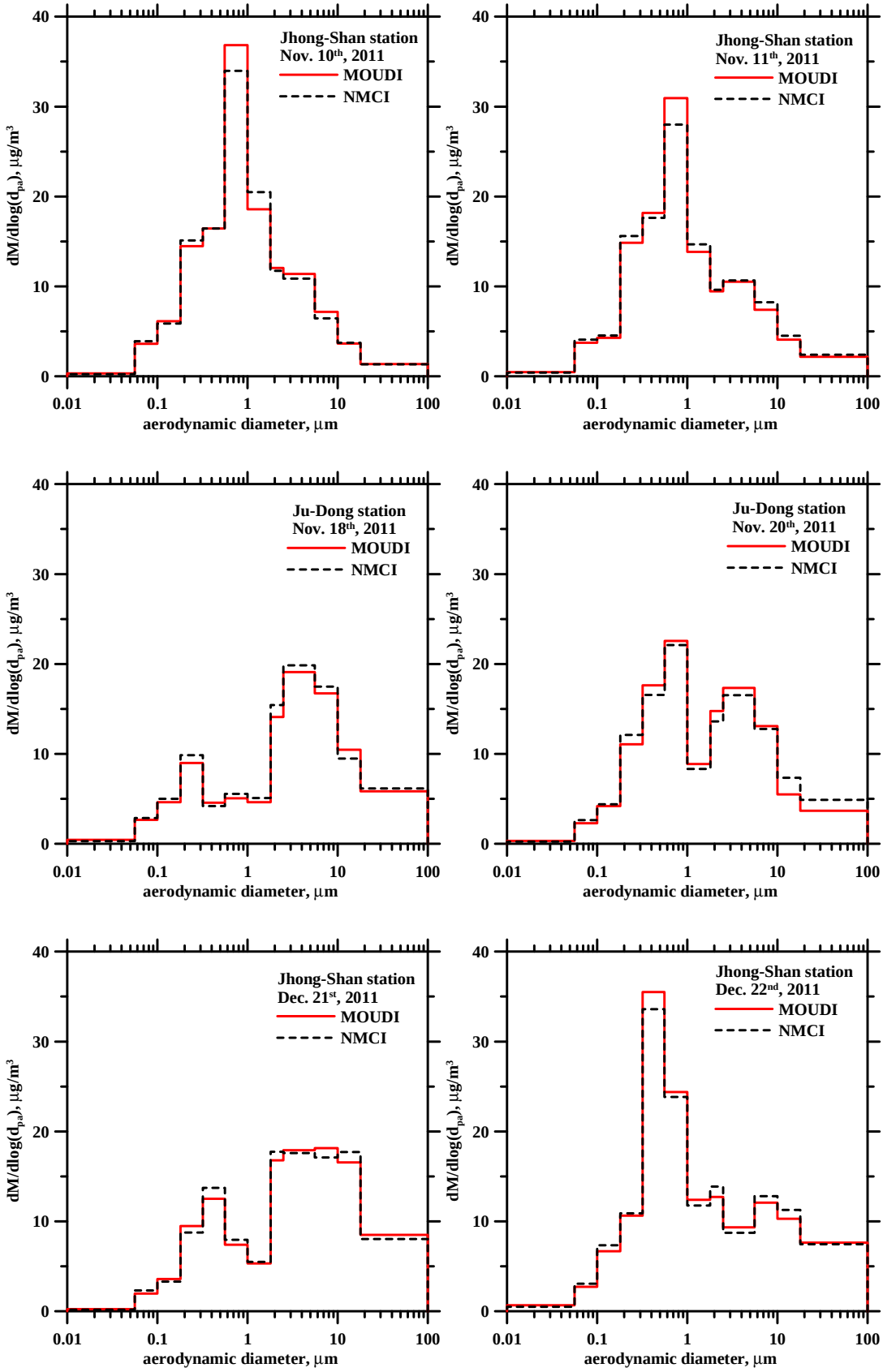

Figure 14 Ambient aerosol mass size distributions measured by the NMCI and the collocated MOUDI.

Figure 15 shows the results of nozzle clogging test expressed in terms of the variation of pressure drop (∆P) across the inlet to 7th or the 8th to 9th stage of the NMCI and the MOUDI during sampling of high concentration incense smokes for 45 min. It can be clearly seen that ∆P increase in the MOUDI is significantly higher than that of the NMCI across the 8th to 9th stage. That means particle clogging in the 8th and 9th stage nozzles of the former is more severe than those of the latter. Micrographs shown in Figure 16 provide further evidence of nozzle clogging in the 7th to 10th stages of the MOUDI while it is much less severe in the NMCI. That is, the new nozzle plates in the lower stages of the NMCI outperform those of the MOUDI in preventing nozzle clogging.

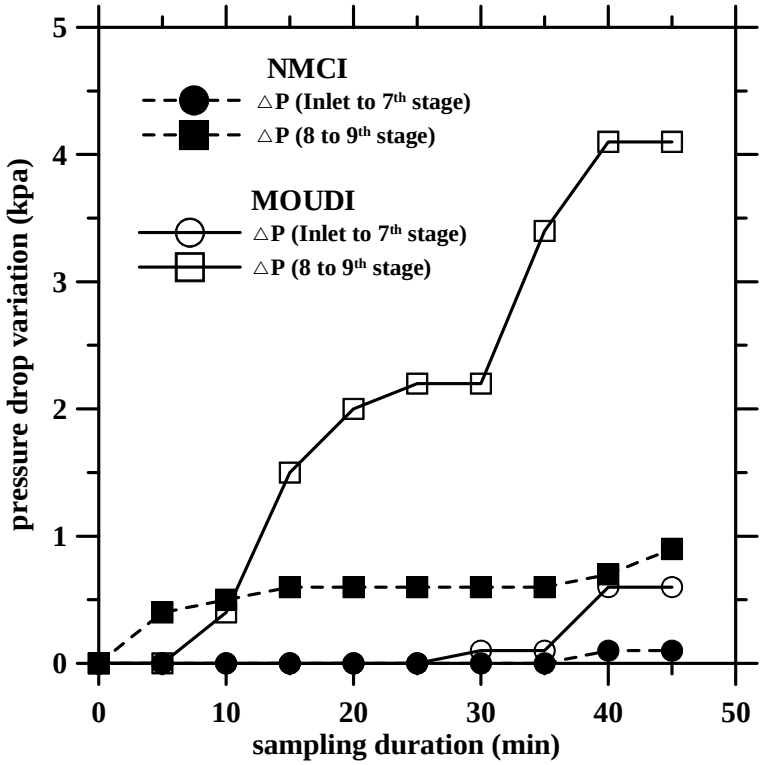

Figure 15 Variation of pressure drop in the MOUDI and the NMCI during sampling of high concentration (25 mg/m^3) incense smokes for 45 min.

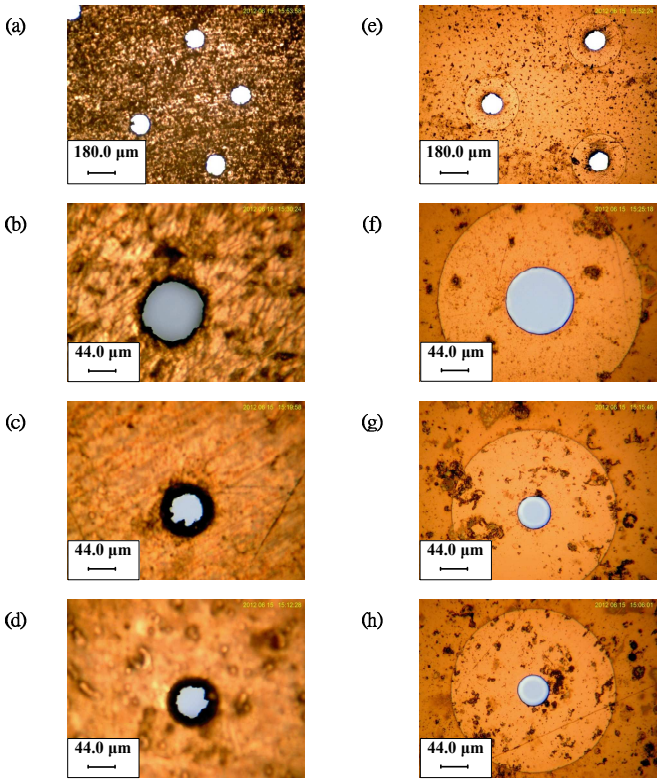

Figure 16 Micrograph of the 7th to 10th [(a) to (d)] stage nozzles of the MOUDI and the 7th to 10th [(e) to (h)] stage nozzles of the NMCI after incense smoke sampling.

4. Conclusion

Particle bounce at different RHs in the commonly used MOUDI was studied in this study by using a humidity control system. The RH of incoming aerosols could be adjusted to 10-98% with ±2% RH by the system. The effect of MOUDI using different impaction substrates, including silicone grease coated ALs (M1), uncoated ALs (M2) and uncoated TFs (M3), on particle bounce was also examined. Particle loss in the humidity conditioner was tested and results showed that it had a very low loss for both $PM_{0.1}$ and $PM_{2.5}$ of less than 5% while slightly high loss for coarse particles ($PM_{2.5-10}$) of about 10% was observed.

M2 oversampled $PM_{0.1}$ mass by 95 and 180% at RH of 50 and 25%, respectively, while those of M3 were 25 and 55%. M2 oversampled $PM_{0.1}$ more severely than M3 at the same RH due to more rigid surface of ALs than TFs .The ambient accumulation mode particles can be collected accurately by the MOUDI as RH >40% even uncoated substrates are used. Coarse particles ($PM_{2.5-10}$) easily get bounce in M2 and M3 when RH <80%, who usually lost in the MOUDI inner wall. On the other hand, particles smaller than 2.5 µm ($PM_{2.5}$) get bounce in M2 and M3 at RH of <~70% and normally be collected in the lower stages when leads to the oversampling of $PM_{0.1}$ but without affecting the concentration of $PM_{2.5}$.

Based on the present experimental results and Fang et al. (1991) who found flow-induced humidity changes on size cut was negligible at RH <80%, it is concluded accurate $PM_{2.5}$ and $PM_{0.1}$ can be obtained with less than 5 % of error at RHs of 65-80% and 75-80% by using uncoated TFs and uncoated ALs in MOUDIs, respectively. The optimal RH can be achieved in 5 min by using the present humidity control system which has a negligible loss for fine particles and UFPs.

Although elevating RH to reduce bounce could lead to shifting the size distribution of sampling particles, Vasiliou et al. (1999) reported that particles are sampled at a known RH then its size distribution at other RHs can be obtained if the dependence of size on RH is known. The relationship between particle size and RH can be measured by the TDMA or calculated using thermodynamic models. Besides, the relationship also can be determined by the present humidity control system.

To avoid possible particle clogging in the nozzles, new nozzle plates with smooth shaped nozzles were fabricated by the LIGA process. The micro-orifice cascade impactor using the new nozzle plates in the 7^{th} to 10^{th} stages (NMCI) and the MOUDI were studied for the particle collection efficiency and nanoparticle interstage loss. In addition, field comparison and nozzle clogging tests were conducted. Calibration results show that after adjusting the S/W ratios to proper values, the d_{pa50} of the 7^{th} to 10^{th} stage of the NMCI and those of the MOUDI are very close to the nominal values given in Marple et al. (1991). It is also found that the d_{pa50} of the nanoparticle stages (9^{th} and 10^{th}) of the MOUDI obtained from the single stage calibration will decrease by 9.4 and 15.4 %, respectively, if all upstream stages are present.

For both impactors, a significant total interstage loss of nanoparticles from inlet to one of the lower stages (7^{th} to 10^{th}) exists especially for nanoparticles with d_{pa} smaller than 40 nm. For nanoparticles larger than 40 nm, the total interstage loss is less than 10 % and it decreases with increasing particle diameter. It is therefore important to consider the nanoparticle loss in the 10^{th} stage of the cascade impactors when determining the mass distributions of nanoparticles. If the size distribution of nanoparticles smaller than 56 nm is to be determined by using the instrument such as the 13-stage MOUDI-II (MSP, Model 122 or 125), nanoparticle loss in the stages 11 to 13 is expected to be even more severe and warrants further investigation.

Field sampling results show that the mass size distributions measured by the NMCI agree well with those of the MOUDI. The nozzle clogging test further indicates that the NMCI outperforms the MOUDI in preventing possible nozzle clogging. In addition, the present NMCI has a sturdy nozzle structure, which allows ultra-sonication of the plates for better cleaning efficiency to remove deposited particles in the nozzles. It is expected that the NMCI can facilitate the accurate size-classified measurements of nanoparticles in the future.

5. Reference

Cass, G. R., Hughes, L. A., Bhave, P., Kleeman, M. J., Allen, J. O., and Salmon, L. G. (2000). The Chemical Composition of Atmospheric Ultrafine Particles, *Philos. Trans. R. Soc. London, Ser. A.* 358:2581–2592.

Chen, S.C., Tsai, C.J., Chou, C.K., Roam, G.D., Cheng, S.S., and Wang, Y.N. (2010a). Ultrafine Particles at Three Different Sampling Locations in Taiwan, *Atmos. Environ.* in press, doi:10.1016/j.atmosenv.

Chow, J.C., Watson, J.G. (2007). Review of measurement methods and compositions for ultrafine particles. *Aerosol Air Quali. Res*. 7: 121–173.

Chen, S.C., Tsai, C.J., Huang, C.Y., Chen, H.D., Chen, S.J., Lin, C.C., Chou, Charles C-K, Lung, S.C., Roam, G.D., Wu, W.Y., Smolik, J., and Dzumbova, L. (2010b). Chemical Mass Closure and Chemical Characteristics of Ambient $PM_{0.1}$, $PM_{2.5}$ and PM_{10} in a Highway Tunnel and at a Roadside. *Aerosol Sci. Technol.* in press.

Chow, J. C., and Watson, J. G. (2007). Survey of Measurement and Composition of Ultrafine Particles, *Aerosol Air Qual. Res.* 7:121–173.

Donaldson, K., Brown, D., Clouter, A., Duffin, R., MacNee, W., Renwick, L., Tran, L., and Stone, V. (2002). The Pulmonary toxicology of Ultrafine Particles, *Journal of Aerosol Medicine—Deposition Clearance and Effects in the Lung.* 15:213–220.

Dzubay, T. G., Hines, L. E., and Stevens, R. K. (1976). Particle Bounce Errors in Cascade Impactor, *Atmos. Environ.* 10:229–234.

Gilmour, M. I., McGee, J., Duvall, R. M., Dailey, L., Daniels, M., Boykin, E., Cho, S.-H., Doerfler, D., Gordon, T., and Devlin, R. B. (2007). Comparative Toxicity of Size-Fractionated Airborne Particulate Matter Obtained from Different Cities in the United States, *Inhal. Toxicol.* 19(Suppl. 1):7–16.

Gormley, P. G., and Kennedy, M. (1949). Diffusion from a Stream Flowing through a Cylindrical Tube, *Proc. Royal Irish Acad*. 52(A):163–169.

Gulijk, C. V., Marijnissen J. C. M., Makkee M., and Moulijn J. A. (2003). Technical Note Oil-soaked Sintered Impactors for the ELPI in Diesel Particulate Measurements, *J. Aerosol Sci.* 34:635–640.

Hering, S.V., Flagan, R.C., Friedlander, S.K., Collins, J.J., Richards, L.W. (1979). Design and evaluation of new low-pressure impactor II. *Environ. Sci. Technol.* 13: 184–188.

Hillamo, R.E., Kauppinen, E.I. (1991). On the Performance of the Berner low pressure impactor. *Aerosol Sci. Technol.* 14: 33–47.

Hinds, W. (1999). *Aerosol Technology: Properties, Behavior, and Measurement of Airborne Particles, Second Edition*. John Wiley & Sons, New York, p. 307–312.

Ji, J. H., Bae, G. N., Hwang, J. (2006). Observation evaluation of nozzle clogging in a micro-orifice impactor used for atmospheric aerosol sampling. *Particulate Science and Technology,* 24:85-96

Keskinen, J., Pietarinen, K., Lehtimaki, M. (1992). Electrical low pressure impactor. *J. Aerosol Sci.* 23: 353–360.

Khlystov, A., Stanier, C., and Pandis, S.N. (2004). An Algorithm for Combining Electrical Mobility and Aerodynamic Size Ddistributions Data When Measuring Ambient Aerosol. *Aerosol Sci. Technol.* 38(S1):229–238.

Liu, C.N., Chen, S.C., Tsai, C.J. (2011). A novel multi-filter PM_{10}–$PM_{2.5}$ sampler (MFPPS). *Aerosol Sci. Technol.* 45: 1480–1487.

Marple, V. A., Robow, K. L., and Behm, S. M. (1991). A Microorifice Uniform Deposit Impactor (MOUDI): Description, Calibration, and Use, *Aerosol Sci. Technol.* 14:434–446.

Marple V.A., Rubow, K.L., Olson, B.A. (2001). Inertial, gravitational, centrifugal, and thermal collection techniques, in: Baron, P.A., Willeke, K. (Eds.), Aerosol measurement: principles, techniques and applications, Wiley Interscience, New York, pp. 229–260.

MSP Corporation (2006). Model 100/110 MOUDI^{TM} user guide, Shoreview, Minnesota.

Oberdörster, G., Oberdorster, E., and Oberdorster, J. (2005). Nanotoxicology: An Emerging Discipline Evolving from Studies of Ultrafine Particles, *Environ. Health Perspectives.* 113:823–839.

Pak, S. S., Liu, B. Y. H., and Rubow, K. L. (1992). Effect of Coating Thickness on Particle Bounce in Inertial Impactor, *Aerosol Sci. Technol.* 16:141–150.

Peters, A., Wichmann, H. E., Tuch, T., Heinrich, J., and Heyder, J. (1997). Respiratory Effects are Associated with the Number of Ultrafine Particles, *Am. J. Respir. Crit. Care Med.* 155:1376–1383.

Peters, T.M., Vanderpool, R.W., Wiener, R.W. (2001). Design and calibration of the EPA $PM_{2.5}$ well impactor ninety-six (WINS). *Aerosol Sci. Technol.* 34: 389–397.

Pui, D.Y.H., Liu, B.Y.H. (1979). Electrical aerosol analyzer: Calibration and performance, in: Lundgren, D.A. et al. (Eds.), Aerosol measurement, University of Florida Press, Gainesville, Florida, pp. 384–399.

Shen, S., Jaques, P.A., Zhu, Y., Geller, M.D., and Sioutas, C. (2002). Evaluation of the SMPS-APS System as a Continuous Monitor for Measuring $PM_{2.5}$, PM_{10} and Coarse ($PM_{2.5-10}$) Concentration, *Atmos. Environ.* 36:3939–3950.

Spencer, M. T., Shields, L. G., and Prather, K. A. (2007). Simultaneous Measurements of the Effective Density and Chemical Composition of Ambient Aerosol Particles, *Environ. Sci. Technol.* 41:1303–1309.

Stein, S.W., Turpin, B.J., Cai, X.P., Huang, C.P.F., and McMurry, P.H. (1994).

Measurements of Relative Humidity-Dependent Bounce and Density for Atmospheric Particles Using the DMA-Impactor Technique, *Atmos. Environ.* 28:1739–1746.

Tsai, C.J. and Cheng, Y.H. (1995). Solid Particle Collection Characteristics on Impaction Surfaces of Different Designs, *Aerosol Sci. Technol.* 23:96–106.

Turner, J. R. and Hering, S. V., (1987). Greased and Ooiled Substrates as Bounce-Free Impaction Surfaces, *J. Aerosol Sci.* 18:215–224.

Tsai, C.J., Liu, C.N., Hung, S.M., Chen, S.C., Uang, S.N., Cheng, Y.S., Zhou, Y. (2012). Novel active personal nanoparticle sampler for the exposure assessment of nanoparticles in workplaces. *Environ. Sci. Technol.* 46: 4546–4552.

U.S Environmental Protection Agency. (2006). National Ambient Air Quality Standards for Particulate Matter; Final Rule, *Fed. Reg.* 71:61144–61233.

Vasiliou, J. G., Sorensen, D. and McMurry, P. H., (1999). Sampling at Controlled Relative Humidity with a Cascade Impactor, *Atmos. Environ.*33:1049–1056.

Virtanen, A., Marjamäki, M, Ristimäki, J., Keskinen, J. (2001). Fine particle losses in electrical low-pressure impactor. *J. Aerosol Sci*. 32: 389–401.

計畫成果自評

相關研究已發表五篇期刊論文，可謂成果豐碩，論文如下：

1. Chen, Sheng-Chieh, Chuen-Jinn Tsai, Cheng-Yu Huang, Hong-Dar Chen, Shui-Jen Chen, Chih-Chung Lin, Jen-Hsiung Tsai, Charles C.K. Chou, S.-C. Candice Lung, Wei-Ru Huang, Gwo-Dong Roam, Wan-Yi Wu, Jiri Smolik, and Lucie Dzumbova. (2010). Chemical Mass Closure and Chemical Characteristics of Ambient Ultrafine Particles and other PM Fractions in a Highway Tunnel and at a Roadside, Aerosol Science and Technology (in press). (SCI), IF=2.686.

2. Chen, Sheng-Chieh, Chuen-Jinn Tsai, Charles C.K. Chou, Sen-Sung Cheng, and Ya-Nan Wang. (2010). Ultrafine particles at three different sampling locations in Taiwan, Atmospheric Environment. Vol. 44, pp. 533-540. (SCI), IF=2.89.

3. Zhu, Chong-Shu, Cheng-Chieh Chen, Jun-Ji Cao, Chuen-Jinn Tsai, Charles C-K Chou, Shaw-Chen Liu, and Gwo-Dong Roam. (2010) Characterization of carbon fractions for atmospheric fine particles and nanoparticles in a highway tunnel. Atmospheric Environment. IF=2.89. (SCI)

4. Chen, S.C., Tsai, C.J., Huang, C.Y., Chen, H.D., Chen, S.J., Lin, C.C., Chou, Charles C-K, Lung, S.C., Roam, G.D., Wu, W.Y., Smolik, J., and Dzumbova, L. (2011). The Influence of Relative Humidity on Nanoparticle Concentration and Particle Mass Distribution Measurements by the MOUDI. *Aerosol Sci. Technol.*, 45(5):713-723.

5. Liu, C.N., Amit, A., Tsai, C.J. (2012). Collection efficiency and interstage loss of nanoparticles in the micro-orifice-based cascade impactor. *Atmos. Environ.*, (submitted).